

HST/STIS UV Spectroscopy of Two Quiescent X-ray Novae: A0620-00 and Centaurus X-4

Jeffrey E. McClintock
Harvard-Smithsonian Center for Astrophysics
60 Garden St., Cambridge, MA 02138
jem@cfa.harvard.edu

and

Ronald A. Remillard
Center for Space Research, MIT
Cambridge, MA 02139
rr@space.mit.edu

ABSTRACT

In 1998 we made UV spectroscopic observations with HST/STIS of A0620-00 and Cen X-4, which are two X-ray novae (aka soft X-ray transients). These binary systems are similar in all respects except that the former contains a black hole and the latter contains a neutron star. A UV spectrum (1700-3100Å) is presented for the quiescent state of each system in the context of previously published UV/optical and X-ray data. The non-stellar, continuum spectrum of black hole A0620-00 has a prominent UV/optical peak centered at $\sim 3500\text{\AA}$. In contrast the spectrum of neutron-star Cen X-4 lacks a peak and rises steadily with frequency over the entire UV/optical band. In the optical, the two systems are comparably luminous. However, black hole A0620-00 is ~ 6 times less luminous at 1700\AA , and ~ 40 times less luminous in the X-ray band. The broadband spectrum of A0620-00 is discussed in terms of the advection-dominated accretion flow model.

Subject headings: black hole physics – accretion, accretion disks – stars: individual (A0620-00; Cen X-4) – X-rays: stars

¹Based on observations with the NASA/ESA *Hubble Space Telescope* obtained at the Space Telescope Science Institute, which is operated by the Association of Universities for Research in Astronomy, Inc., under NASA contract NAS5-26555.

1. Introduction

In the fall of 1975, the X-ray nova A0620-00 reached an intensity of 50 Crab to become the brightest (non-solar) celestial X-ray source that has ever been observed. After the system returned to quiescence in the fall of 1976, it was found to be a 7.8 hr binary containing a K5 dwarf secondary and a non-stellar continuum source, which was attributed to an accretion disk (Oke 1977; McClintock et al. 1983). The brightness of the quiescent optical counterpart ($V = 18.3$) and the low mass of the secondary motivated a radial velocity study which led to the discovery of the first black-hole primary in an X-ray nova (McClintock & Remillard 1986).

Already in 1981, the quiescent X-ray source was known to be extraordinarily faint with $L_x < 10^{-6}L_{max}$ (Long et al. 1981). McClintock (1986) noted that this faintness posed the following puzzle: By close analogy with dwarf novae, A0620-00’s quiescent accretion disk ($M_V \sim 7$) implied a mass accretion rate of $\dot{M} \sim 10^{-11} M_\odot \text{ yr}^{-1}$. Thus, if one assumed the canonical efficiency of $\sim 10\%$ for converting gravitational energy into radiant energy, then one would expect the source to be ~ 1000 brighter in X-rays than was observed.

A few explanations for the lack of X-rays were suggested (e.g. de Kool 1988; Huang and Wheeler 1989), but none was satisfactory. Moreover, these suggestions were overtaken by the advection-dominated accretion flow (ADAF) model (Narayan & Yi 1994, 1995, and references therein). An early application of the ADAF model by Narayan, McClintock, and Yi (1996) showed that it could account naturally for both the broadband spectrum of A0620-00 and for its minuscule X-ray luminosity of $\approx 6 \times 10^{30} \text{ ergs s}^{-1}$ (McClintock, Horne & Remillard 1995; hereafter MHR95).

Similar fits were made successfully to the broadband spectra of other quiescent X-ray novae (Narayan, Barret, & McClintock 1997a; Hameury et al. 1997). The results presented herein are discussed in terms of these spectra and the ADAF model, which is based on the idea that at low \dot{M} the gravitational potential energy released in an accretion flow may be stored as thermal energy rather than being radiated. An ADAF flow is optically thin, nearly radial, and extraordinarily hot near the compact object. Thus in the case of a black hole, nearly all of the gravitational energy can be advected through the event horizon and swallowed by the hole, thereby accounting for the tiny X-ray luminosity of A0620-00 quoted above. On the other hand, a neutron star accreting via an ADAF is expected to be much more luminous for the same \dot{M} because the accreting gas will strike the surface and heat the star (assuming it is not deflected by the propeller effect), thereby converting gravitational energy into radiation with the canonical efficiency of $\sim 10\%$ (Narayan, Garcia, & McClintock 1997b; Menou et al. 1999).

We reported earlier on a UV spectrum of A0620-00 of modest quality that was obtained with the FOS during HST Cycle 1 (MHR95). Here we report on UV spectra of both A0620-00 and Cen X-4 that are of excellent quality and were obtained in 1998 with the STIS during Cycle 7. The UV spectrum of Cen X-4 in quiescence is the first such spectrum of this object to be published.

Cen X-4 is a type I burst source and therefore contains a neutron star primary, which is only

about 15% as massive as the black hole primary in A0620-00 (Shahbaz, Naylor, & Charles 1994). The quiescent X-ray luminosity of Cen X-4, $L_x \sim 2.5 \times 10^{32}$ ergs s⁻¹, is ~ 40 times larger than the X-ray luminosity of A0620-00 (Asai et al. 1998; MHR95). In most other respects, however, Cen X-4 and A0620-00 are very similar. For example, the orbital period of Cen X-4 is 15.1 hrs *vs.* 7.8 hrs for A0620-00, and so their predicted mass transfer rates are quite comparable (Menou et al. 1999). Their estimated distances are about the same: 1.2 kpc (Chevalier et al. 1989; Barret, McClintock, & Grindlay 1996). Both systems contain K-dwarf secondaries, and both are known to have erupted twice: Cen X-4 in 1969 and 1979, and A0620-00 in 1917 and 1975.

2. Observations and Analysis

We report on eight UV spectra of A0620-00 (V616 Mon) and one UV spectrum of Cen X-4 (V822 Cen) that were obtained with the HST/STIS spectrograph. Some details of the observations are presented in Table 1. All of the observations employed the G230L grating, the clear filter, the 52" x 0.5" aperture and the NUV-MAMA detector. The spectral resolution is 3.2Å (FWHM). The data were recorded in the “time-tagged” mode.

Our results presented herein are based on the calibrated “pipeline” spectral data provided to us by STScI. We converted each of the “1-D” table files into several 1-D IRAF spectra containing the flux, the error in the flux, the background, etc. The first UV spectrum obtained for A0620-00 (entry 2 in Table 1) has a high background level and we rejected it; no problems were found with the remaining spectra. Thus, the single spectrum of A0620-00 presented herein is a sum of seven individual spectra (entries 3-6 and 9-11 in Table 1) with a total exposure time of 4.8 hours. Only a single spectrum was obtained of Cen X-4 (Table 1, entry 8); the exposure time was 0.6 hours.

The fluxes were dereddened using the interstellar extinction law of Cardelli, Clayton & Mathis (1989). For A0620-00 we adopted a reddening of $E(B-V) = 0.35$ (Wu et al. 1983; also, see Oke & Greenstein 1977). For Cen X-4 we used $E(B-V) = 0.10$ (Blair et al. 1984). The uncertainty in the reddening of either source probably does not exceed 0.05 mag (Wu et al. 1976, 1983; Blair et al. 1984). In §3.4 we illustrate the effects of this uncertainty on our UV spectra.

To confirm that A0620-00 and Cen X-4 were quiescent near the time of the STIS observations, we obtained V-band CCD images of both fields using the FLWO 1.2m telescope at Mt. Hopkins, AZ. As Table 1 shows, these optical observations occurred about 11 hours before the STIS observation of Cen X-4 and about 25 hours before the longer sequence of observations of A0620-00. The airmass and seeing were, respectively, 1.3 and 2.5" for the observations of A0620-00 and 2.2 and 2" for CenX-4. The sky was clear during the observations of both objects. All of the data were reduced in the standard way using bias frames, dome flats and the NOAO IRAF reduction package. The absolute calibration for A0620-00 was derived from Landolt (1992) stars in four fields, which were observed throughout the night. The absolute calibration for Cen X-4 was obtained from the magnitudes of two nearby comparison stars (Chevalier et al. 1989).

We also present new results on the V-band optical variability of A0620-00 based on the following data collected by us: (1) One 20-min CCD image was obtained on 1992 February 5.156 UT using the McGraw-Hill 1.3m telescope; (2) one 10-min image was obtained on 1992 April 7.006 UT using the CTIO 1.5m telescope; and (3) 23 images were obtained during four nights—1995 December 21 and 1996 January 13–15—using the FLWO 1.2m telescope. In all cases, the data reduction and analysis were performed using IRAF. The absolute calibration relies on the magnitudes of three nearby field stars, which were derived from the 1998 March 3 observation of A0620-00 described above.

3. Results

3.1. Spectra of A0620-00 and Cen X-4

The spectra of A0620-00 and Cen X-4 are shown in Figure 1a. No correction has been applied for interstellar reddening. The prominent emission feature in both spectra is Mg II $\lambda\lambda 2796, 2803$. For A0620-00, the line has the same equivalent width (EW) on 1998 March 4 and on May 5 (Table 1): $174 \pm 8 \text{ \AA}$. Similarly, the line width is the same for both observations of A0620-00: $23 \pm 2 \text{ \AA}$ (FWHM), where a small correction has been applied for the 3.2 \AA spectral resolution of the STIS. For Cen X-4, the EW of the Mg II line is $63 \pm 5 \text{ \AA}$ and the line width corrected for instrumental resolution is $13.5 \pm 2.0 \text{ \AA}$ (FWHM). Another significant emission feature, which is also present in both spectra, is Fe II $\lambda\lambda 2586 - 2631$. Both the Mg II and Fe II emission lines appear with comparable EWs in the 1992 spectrum of A0620-00 (MHR95).

The continuum for A0620-00 is faint and steadily decreases with wavelength to $f_\lambda \lesssim 6 \times 10^{-18} \text{ ergs s}^{-1} \text{ cm}^{-2} \text{ \AA}^{-1}$ for $\lambda \lesssim 2300 \text{ \AA}$. The faint continuum is due partly to the cutoff in the source spectrum at short wavelengths (as illustrated below), and partly to extinction ($E_{B-V} = 0.35$). On the other hand, the observed continuum spectrum of Cen X-4 is relatively flat over the entire range and actually rises somewhat with decreasing wavelength (Fig. 1b).

3.2. Optical and X-ray Variability of Cen X-4 and A0620-00

The quiescent optical counterparts of both A0620-00 and Cen X-4 are modulated at their orbital periods with semiamplitudes of ≈ 0.1 mag. The mean brightness of Cen X-4, however, varies by much more than this. Chevalier et al. (1989) report on 570 V-band measurements obtained over a 3-year period. During most observing runs they found $V \approx 18.6 - 18.2$. However, they frequently found that the counterpart brightened further to $V \approx 18.1 - 17.7$, which they call the “active state.” Occasionally, the variations occurred from night to night, but usually they occurred on a longer time scale. Similar variability in B and B-V was extensively observed by Cowley et al. (1988). Furthermore, despite the paucity of X-ray measurements, the quiescent

X-ray flux of Cen X-4 has been observed to vary by a factor of 3 in less than four days (Campana et al. 1997). Thus, both the V-band and X-ray intensity of Cen X-4 have been observed to vary by a factor of $\sim 2 - 3$ on time scales of a day or longer. Our V-band observation of Cen X-4, which was performed shortly before our STIS observation (Table 1, entries 7-8), gave $V = 18.2 \pm 0.1$, which is consistent with values reported for the quiescent state (e.g. $V = 18.6-18.2$; Chevalier et al. 1989).

No comparable degree of variability has been reported for A0620-00 in quiescence. The earliest value for the quiescent V magnitude is given by Oke (1977): $V = 18.35$ on 1976 November 15-17. Here we report in chronological order a number of new results (see §2): (1) $V = 18.20 \pm 0.05$ on 1992 February 5.156 UT; (2) $V = 18.20 \pm 0.05$ on 1992 April 7.006 UT; (3) $\bar{V} = 18.25 \pm 0.08$ ($n = 23$) on 1995 December 21 and 1996 January 13-15, where the uncertainty is the sample standard deviation, and the mean magnitude is consistent with the mean magnitudes computed for each of the four individual nights; and (4) $V = 18.37 \pm 0.05$ on 1998 March 3 (see Table 1). Thus, apart from orbital modulation, the mean magnitude of A0620-00 appears to be relatively stable: $\bar{V} \approx 18.3$. There is no useful data on possible X-ray variability. Therefore, based on the very limited data available for A0620-00 in quiescence, we tentatively conclude that the mean magnitude of its optical counterpart is significantly less variable ($\overline{\Delta V} \approx 0.1$ mag) than the quiescent counterpart of Cen X-4 ($\overline{\Delta V} \approx 1$ mag).

3.3. Ultraviolet Variability and Reddening of A0620-00

The STIS spectra of A0620-00 obtained two months apart provide strong evidence for UV variability. The March 4 and May 5 spectra (Table 1), excluding the Mg II line, are compared in Figure 2. The STIS flux value in a particular 100\AA band is the mean of three flux measurements for the May 5 data and the mean of four measurements for the March 4 data (see Table 1). The uncertainty in a given band is the sample standard deviation of the (3 or 4) flux measurements in that band. Here and elsewhere we use the standard deviation because it provides a realistic estimate of the random error which includes the effects of source variability and counting statistics.

The uncertainties shown in Figure 2 (for $2400\text{\AA} \leq \lambda \leq 3000\text{\AA}$) are typically 12%, whereas the uncertainties due to counting statistics are much smaller ($\sim 3\%$). This implies that A0620-00 varies by $\sim 12\%$ on a time scale of one 90-min HST orbit. (For evidence of variability on a time scale of minutes, see §2.2 in MHR95.)

Comparing the nominal spectra plotted in Figure 2, we conclude that the continuum flux ($2250 < \lambda < 3150\text{\AA}$) decreased by a factor of ≈ 1.25 in 1998 between March 4 and May 5. We have ignored the 4% uncertainty in the calibration and stability of the STIS with its MAMA detector (STIS Instrument Handbook, Vers. 2.0).

Given the significant reddening of A0620-00, $E(B-V) \approx 0.35$ mag, we examined the spectra for evidence of absorption near 2200\AA . The March 4 spectrum shown in Figure 2 contains such a

feature. We examined the significance of this broad feature by binning the data in 50\AA intervals and restricting our attention to the wavelength range $1900\text{-}2600\text{\AA}$. We corrected this spectrum for increasing amounts of IS reddening corresponding to $E(B-V) = 0.1, 0.2, 0.3$, etc. (Cardelli et al. 1989). For each of these data sets, the uncertainties in the fluxes were represented by the sample standard deviation, as in Figure 2. In the usual way, we fitted the corrected data sets to power law spectra ($F_\lambda \sim \lambda^n$) and computed χ^2 vs. $E(B-V)$. Acceptable fits (i.e. data sets with $\chi^2 \sim 1$ and a weak absorption feature) were obtained for $0.3 \lesssim E(B-V) \lesssim 0.7$, with a best value near 0.5. This value is consistent with the one determined by Wu et al. (1976,1983) during the 1975 outburst of A0620-00 (see §2); however, our value is much less precise due to the variability and faintness of the quiescent source. For the fainter May 5 spectrum (Fig. 2), no 2200\AA feature is evident; in fact, no significant flux was detected for $\lambda \leq 2200\text{\AA}$.

3.4. A Comparison of the UV/Optical Spectra of A0620-00 and Cen X-4

The spectra of the two sources corrected for reddening are compared in Figure 3ab. To facilitate our analysis of the STIS continuum spectra, we have clipped out the Mg II and Fe II emission lines and averaged the spectra in 100\AA intervals. Reddening corrections have been applied and the results are expressed in units of $\log(\nu F_\nu)$ vs. $\log(\nu)$, which have been used extensively in modeling the spectra of X-ray novae (e.g. Narayan et al. 1997a). The STIS fluxes and the V-band fluxes reported here are plotted as filled circles. The effects on the STIS spectra of varying the reddening by ± 0.05 mag from the nominal values are indicated by the flanking histograms. In the spectrum of A0620-00 (Fig. 3a), FOS UV/optical fluxes obtained six years earlier and some additional optical data for $\lambda \geq 5000\text{\AA}$ are plotted as open squares (see Narayan et al. 1996, and references therein). All of the longer wavelength flux data ($\lambda \gtrsim 3500\text{\AA}$) shown here is non-stellar: i.e. the data have been corrected by subtracting an approximate contribution due to the K-dwarf secondary (see below).

For A0620-00 (Fig. 2a), a factor of 2.0 discrepancy in flux level is evident in the $2400\text{-}3000\text{\AA}$ overlap range between the 1992 FOS spectrum and the 1998 STIS spectrum. As noted in §3.3, the absolute photometric accuracy of the STIS data are 4%. Thus the only simple explanations for the offset between the spectra are (1) the FOS fluxes are in error, (2) the source varied or (3) both 1 & 2 are true. We cannot decide this question with the available information. However, we note that the FOS sensitivity in Cycle 1 was handicapped by the pre-COSTAR optics. Furthermore, the source was faint and the FOS provided no direct measure of the background (MHR95). There is one quantitative point that narrows the FOS/STIS discrepancy: In 1992 we observed A0620-00 with two FOS dispersers and found that the “blue prism” fluxes (which we adopted in MHR95 and are shown plotted here in Fig. 3a) exceeded the G160L grating fluxes by $\sim 35\%$ in the $2200\text{-}2400\text{\AA}$ overlap range (MHR95). Had we adopted the grating fluxes (now considered more reliable), the FOS/STIS discrepancy would be a factor of 1.5 instead of 2.0 (as shown in Fig. 3a). On the other hand, source variability may be largely responsible for the discrepancy. Although very little

V-band variability has been observed over 12 years (§3.2), the STIS results do provide strong evidence for a $\sim 25\%$ variation in the UV flux in two months (§3.3 and Fig. 2).

The non-stellar spectrum of A0620-00 at longer wavelengths ($\lambda \gtrsim 3500\text{\AA}$) is somewhat uncertain because one must subtract a large stellar component due to the K-dwarf secondary. Subtracting the spectrum of a K5V field star, Oke (1977) first derived the non-stellar spectrum of A0620-00 (3200-10000 \AA). Specifically, he found that the non-stellar component contributed $43 \pm 6\%$ of the total light in the V-band. We also used a K5 dwarf and a somewhat different technique to obtain very similar results at six later epochs (MHR95). On the other hand, using a K3/4 dwarf, Marsh, Robinson & Wood (1994) found a much smaller contribution for the non-stellar component: $17 \pm 4\%$ at $\sim 4800\text{\AA}$ and $6 \pm 3\%$ at $\sim 6300\text{\AA}$. In Figure 2a, the non-stellar optical spectrum based on Oke’s decomposition is plotted as open squares. The dashed line indicates approximately the effect on Oke’s spectrum of applying the results of Marsh et al. (1994), which call for a ~ 3 -fold decrease in the non-stellar spectrum at 4800\AA and a ~ 6 -fold decrease at 6300\AA , as indicated by the pair of open triangles in Fig. 3a. The difference between the two optical spectra is most likely due to the choice of a proxy star to represent the secondary of A0620-00. Marsh et al. chose a hotter star with weaker lines (K3/4 *vs.* K5), which would be expected to give a smaller non-stellar contribution. In any case, we tentatively conclude that the optical spectrum of the non-thermal radiation is relatively uncertain, but it is very probably bounded by the open squares and dashed line in Fig. 3a.

For A0620-00, the total V magnitude was the same for Oke in 1976 as it was for us in 1998 (see §3.2). Thus in plotting this data point in Figure 3a, we have assumed that the fraction of non-stellar light is 43%, as derived by Oke (1977). For Cen X-4 at V (Fig. 3b), we have assumed nominally that 30% of the total light (corresponding to $V = 18.2$; see §3.2) is non-stellar; the liberal error bar assumes that the non-stellar fraction is within the range 0.25-0.40 (Chevalier et al. 1989; McClintock & Remillard 1990; Shahbaz, Naylor & Charles 1993).

The key result of Figure 3ab comes from comparing the reliable STIS spectra of A0620-00 and Cen X-4 in the range 1800-3100 \AA . The absolute photometric accuracy of these spectra is 4% (§3.3), and they are not at all affected by “light pollution” from the cool secondary stars. *These spectra are strikingly different: The intensity of A0620-00 decreases by a factor of ~ 3 in the interval 1900-3000 \AA ($15.0 < \log(\nu) < 15.2$). In contrast, the intensity of Cen X-4 rises with frequency over the entire observed UV band.*

3.5. The Broadband Spectra of A0620-00 and Cen X-4 Compared

The spectra of both sources are shown in Figure 4ab extending from the optical to the X-ray. The UV/optical spectrum is the same as shown in Figure 3ab. The upper limit near 50 eV ($\log(\nu) \sim 16.6$) for A0620-00 is deduced from an upper limit on HeII $\lambda 4686$ emission (Marsh et al. 1994; Narayan et al. 1996). For both sources the X-ray data near 5 keV was obtained with ASCA

(Asai et al. 1998). The detection plotted for A0620-00 at 1 keV was obtained with the ROSAT PSPC (MHR95).

For both A0620-00 and Cen X-4, the X-ray data and the UV data were obtained at different epochs. Thus, for Cen X-4 we expect that source variability introduces an uncertainty in this composite spectrum (Fig. 4b) that is about a factor of 3 (see §3.2), which is comparable to the measurement uncertainties for the X-ray data (Asai et al. 1998). Source variability for A0620-00 appears to be less (§3.2) and may affect the UV/X-ray spectrum by a factor $\lesssim 2$, which is somewhat less than the uncertainty in the measured X-ray flux (MHR95). Thus, the appearance of Figure 4ab is unlikely to be affected significantly by source variability.

A key result shown in Figure 4ab is the very different character of the broadband spectra of the two sources in passing from the optical to the X-ray: the flux (νF_ν) of A0620-00 falls by a factor of ~ 70 , whereas, the flux of Cen X-4 decreases by only a factor of 2-3.

4. Discussion

A strong Mg II $\lambda 2800$ emission line is present in the spectra of both A0620-00 and Cen X-4 (Fig. 1; §3.1). Mg II $\lambda 2800$ is especially broad and intense in the spectrum of A0620-00, and it is natural to compare it to H $_\alpha$ in emission, the line that dominates the optical spectrum of A0620-00. The average width of the Mg II line measured for the seven individual spectra is $\text{FWHM} = 2500 \pm 220 \text{ km s}^{-1}$, which is comparable to the width of H $_\alpha$: $\text{FWHM} \approx 2000 \text{ km s}^{-1}$ (Marsh et al. 1994; Orosz et al. 1994). However, the line profiles are very different. The Mg II line is plainly single peaked (Fig. 1a), given the adequate spectral resolution of the STIS (3.2\AA or 340 km s^{-1}); on the other hand, the H $_\alpha$ line is always double peaked. The broad and double-peaked H $_\alpha$ line is ubiquitous in the spectra of quiescent X-ray novae and cataclysmic variables, and is generally attributed to emission from an accretion disk (e.g. Horne & Marsh 1986). We know of no ready explanation for the single-peaked profile of the Mg II line.

It is also interesting to consider for each system the luminosities of the H $_\alpha$ and Mg II lines relative to the X-ray luminosity. For A0620-00 we find (in units of $10^{30} \text{ ergs s}^{-1}$): $L_{\text{H}\alpha} \approx 3.4$, $L_{\text{Mg II}} \approx 3.4$ and $L_x \approx 6$ (Oke 1977; Marsh et al. 1994; Orosz et al. 1994; MHR95). Thus the line and X-ray luminosities are very comparable; plainly the X-ray source is incapable of powering the lines. For Cen X-4 we find: $L_{\text{H}\alpha} \approx 1.2$, $L_{\text{Mg II}} \approx 2.8$ and $L_x \approx 250$ (Shahbaz et al. 1993; Shahbaz et al. 1996; Asai et al. 1998). The line luminosities for the two systems are quite similar, although the X-ray luminosity of Cen X-4 is greater by a factor of ~ 40 . For both systems, we conclude that both the H $_\alpha$ and Mg II lines are very probably produced in an outer accretion disk or gas stream (Horne & Marsh 1986) and are little affected by the radiation from the central X-ray source.

As shown in Figure 4, the flux (νF_ν) of A0620-00 falls by a factor of ≈ 70 in passing from the peak in the UV/optical band to the X-ray band. Comparable data exist for only two other black-hole X-ray novae, and in these cases the (dereddened) UV/optical flux is also much greater

than the X-ray flux: The flux of V404 Cyg decreases by a factor of ≈ 20 (Narayan et al. 1997a) and GRO J1655-40 by a factor of ≈ 50 (Hameury et al. 1997).

Among the black-hole X-ray novae, the break in the UV spectrum for $\log(\nu) \gtrsim 14.9$ is presently observable only for A0620-00 (Fig. 4a) because its IS extinction is moderate, the source is bright, and the cool secondary does not contaminate the UV spectrum. FOS observations of A0620-00 in HST Cycle 1 provided some preliminary evidence for the existence of an optical/UV peak (MHR95; Narayan et al. 1996); however, the results were inconclusive due to serious difficulties in determining the background rate at short wavelengths (MHR95). Now, however, these earlier indications of a break in the spectrum are amply confirmed by the STIS observations reported here. Jointly the FOS and STIS observations establish a peak near $\log(\nu) \sim 14.9$. The flux is seen to fall abruptly by a factor of ≈ 3 in the UV band, and to be ≈ 70 times fainter in the X-ray band (Fig. 4a).

The striking UV/optical peak in the spectrum of A0620-00 (Fig. 4a) has been ascribed in ADAF models to synchrotron emission (Narayan et al. 1996; Narayan et al. 1997a). Since synchrotron emission is a strong function of electron temperature, the bulk of this emission comes from within $\sim 10 R_S$ ($R_S = 2GM/c^2$) of the black hole. ADAF models have yielded good fits to all of the available broadband data (Narayan et al. 1997a; Hameury et al. 1997). That is, the synchrotron peak in the models dominates over the X-ray flux by a factor of $\sim 20 - 70$, as observed. Moreover, at higher energies the observed photon index (0.7-8.5 keV) of V404 Cyg, $\Gamma = 2.1(+0.5, -0.3)$, is well matched by the Compton scattering and bremsstrahlung components of the ADAF model spectrum (Narayan et al. 1997a). In these models, it was assumed that none of the accreting mass was lost to a wind, and also that the fraction of the turbulent energy that goes into heating the electrons is $\delta \sim (m_e/m_i) \sim 10^{-3}$.

At the close of §1, we listed several similarities between A0620-00 and Cen X-4. Several dissimilarities have been pointed out in the present work. The broadband spectrum of Cen X-4 (Fig. 4b) is plainly different. First, compared to A0620-00 and other black-hole X-ray novae, the decrease in the flux of Cen X-4 in going from the UV band to the X-ray band is very small—a factor of ~ 2 (Fig. 4b). Second, there is no peak in the *observed* UV/optical continuum; the spectrum generally increases with increasing frequency. An observational challenge is to search for a break in the UV spectrum of Cen X-4 to the shortest possible wavelengths. This is important since the peak of the thermal synchrotron emission in ADAFs depends on the mass of the compact object: $\nu_s \sim 10^{15}(M/M_\odot)^{-1/2}$ (Quataert & Narayan 1999b). Thus, in relation to the spectrum of A0620-00, the spectrum of Cen X-4 may be expected to peak at wavelengths $\sim 1500\text{\AA}$ (see §1). A corresponding theoretical challenge is to develop ADAF models for quiescent accretion onto neutron stars (Yi et al. 1996). This is a difficult undertaking because a neutron star surface will re-radiate the thermal energy it accretes via an ADAF, making it difficult to observe the faint component of radiation due to the ADAF. A black hole, on the other hand, is much simpler because its event horizon will hide the thermal energy (Narayan et al. 1997b).

From the observational point of view, compelling evidence now exists for a large luminosity difference between black holes and neutron stars at quiescent levels of accretion. Chandra and XMM observations that are now scheduled will soon provide conclusive results on this luminosity divide. In the context of the ADAF model, this luminosity difference provides evidence that black holes possess an event horizon (Narayan et al. 1997b; Garcia et al. 1998; Menou et al. 1999). The results presented here substantiate this earlier work and provide additional information: A0620-00 and Cen X-4 are at very comparable distances and have similar mass transfer rates (§1). Nevertheless, A0620-00 is ~ 40 times less luminous than Cen X-4 in the X-ray band (§1), as expected if A0620-00 has an event horizon and Cen X-4 does not. At $\sim 1700\text{\AA}$ however, A0620-00 is less luminous by only a factor of ~ 6 , and in the optical band, where the observed luminosity is a maximum, the two systems are comparably luminous (Fig. 4).

Recently, the ADAF model has been successfully applied to the spectra of $10^8 - 10^{10} M_{\odot}$ black holes in the nuclei of elliptical galaxies (Di Matteo et al. 1999). The observed spectra of most of these supermassive black holes differ markedly from the spectra of quiescent Galactic black holes in two respects. First, the synchrotron peak is dwarfed by the X-ray peak: For six galactic nuclei, the peak synchrotron flux is typically only a few percent of the peak X-ray flux (Di Matteo et al. 1999). Second, their X-ray spectra are significantly harder than the spectra of BHXN (photon index $\Gamma = 0.6 - 1.5$; Allen, Di Matteo, & Fabian 1999). Consequently, the ADAF models used to fit the supermassive black holes differ significantly from the models applied previously to the Galactic black holes. The fundamental difference in the new models is the presence of a massive wind that can expel much or most of the incoming accretion flow (Narayan & Yi 1994, 1995; Blandford & Begelman 1999). The newer models also consider much stronger heating of the electrons ($\delta \sim 0.01 - 0.75$) (Quataert & Narayan 1999a, 1999b).

Because there is a degeneracy in the parameters, it has been possible to construct new ADAF models for the X-ray nova V404 Cyg with strong winds and large values of δ that are comparable in quality to the earlier fits described above, which were achieved with no winds and $\delta \sim 0.001$ (Quataert & Narayan 1999b; Narayan et al. 1997a). Observations with Chandra and XMM will soon tighten substantially the constraints on the model fits. Obviously, these observations will be crucial to our explorations of both Galactic black holes and supermassive black holes that are accreting via an ADAF. An important goal is to obtain a unified ADAF model for low-luminosity black holes with masses ranging from $10 M_{\odot}$ to $10^{10} M_{\odot}$.

We thank K. Menou, R. Narayan, E. Quataert, G. Sobczak and the referee, K. Long, for helpful discussions and comments on the manuscript; and L. Macri and E. Barton for making contemporaneous V-band observations of our objects; and numerous people at STScI for help with the STIS observations and data analysis, including S. Baum, R. Bohlin, G. Kriss, H. Lanning, K. Peterson, K. Sahu and B. Simon. Support for this work was provided by NASA through grant number GO-07393.01-96A from the Space Telescope Science Institute, which is operated by AURA, Inc., under NASA contract NAS5-26555.

REFERENCES

- Allen, S. W., Di Matteo, T., & Fabian, A. C., 1999, MNRAS, submitted (astro-ph/9905052)
- Asai, K., Dotani, T., Hoshi, R., Tanaka, Y., Robinson, C. R., & Terada, K. 1998, PASJ, 50, 611
- Barret, D., McClintock, J. E., & Grindlay, J. E. 1996, ApJ, 473, 963
- Blair, W. P., Raymond, J. C., Dupree, A. K., Wu, C.-C., Holm, A. V., & Swank, J. H. 1984, ApJ, 278, 270
- Blandford, R. D., & Begelman, M. C. 1999, MNRAS, 303, L1
- Campana, S., Mereghetti, S., Stella, L., & Colpi, M. 1997, A&A, 324, 941
- Cardelli, J. A., Clayton, G. C., & Mathis, J. S. 1989, ApJ, 345, 245
- Chevalier, C., Ilovaisky, S. A., van Paradijs, J., Pedersen, H., & van der Klis, M. 1989, A&A, 210, 114
- Cowley, A. P., Hutchings, J. B., Schmidtke, P. C., Hartwick, F. D. A., Crampton, D., & Thompson, I. B. 1988, AJ, 95, 1231
- de Kool, M. 1988, ApJ, 334, 336
- Di Matteo, T., Quataert, E., Allen, S. W., Narayan, R., & Fabian, A. C. 1999, MNRAS, submitted (astro-ph/9905053)
- Garcia, M. R., McClintock, J. E., Narayan, R., & Callanan, P. 1998, in the Proceedings of the 13th North American Workshop on CVs, eds. S. Howell, E. Kuulkers, & C. Woodward, p. 506 (astro-ph/9708149)
- Horne, K., & Marsh, T. R. 1986, MNRAS, 218, 761
- Huang, M., & Wheeler, J. C. 1989, ApJ, 343, 229
- Landolt, A. U. 1992, AJ, 104, 340
- Long, K. S., Helfand, D. J., & Grabelsky, D. A. 1981, ApJ, 248, 925
- Hameury, J.-M., Lasota, J.-P., McClintock, J.E., & Narayan, R. 1997, ApJ, 489, 234
- Marsh, T. R., Robinson, E. L., & Wood, J. H. 1994, MNRAS, 266, 137
- Menou, K., Esin, A. A., Narayan, R., Garcia, M. R., Lasota, J.-P., & McClintock, J. E. 1999, ApJ, 520, 276
- McClintock, J. E. 1986, in The Physics of Accretion onto Compact Objects, ed. K. O. Mason, M. G. Watson, & N. E. White (Berlin: Springer), 211
- McClintock, J. E., Horne, K., & Remillard, R. A. 1995, ApJ, 442, 358 (MHR95)
- McClintock, J. E., Petro, L. D., Remillard, R. A., & Ricker, G. R. 1983, ApJ, 266, L27
- McClintock, J. E., & Remillard, R. A. 1986, ApJ, 308, 110
- McClintock, J. E., & Remillard, R. A. 1990, ApJ, 350, 386

- Narayan, R., & Yi, I. 1994, ApJ, 428, L13
- Narayan, R., & Yi, I. 1995, ApJ, 452, 710
- Narayan, R., Barret, D., & McClintock, J. E. 1997a, ApJ, 482, 448
- Narayan, R., Garcia, M. R., & McClintock, J. E. 1997b, ApJ, 478, L79
- Narayan, R., McClintock, J. E., & Yi, I. 1996, ApJ, 457, 821
- Oke, J. B. 1977, ApJ, 217, 181
- Oke, J. B., & Greenstein, J. L. 1977, ApJ, 211, 872
- Orosz, J. A., Bailyn, C. D., Remillard, R. A., McClintock, J. E., & Foltz, C. B. 1994, ApJ, 436, 848
- Quataert, E. & Narayan, R. 1999a, ApJ, 516, 399
- Quataert, E. & Narayan, R. 1999b, ApJ, 520, 298
- Shahbaz, T., Naylor, T., & Charles, P. A. 1993, MNRAS, 265, 655
- Shahbaz, T., Naylor, T., & Charles, P. A. 1994, MNRAS, 268, 756
- Shahbaz, T., Smale, A. P., Naylor, T., Charles, P. A., van Paradijs, J., Hassall, B. J. M., & Callanan, P. 1996, MNRAS, 282, 1437
- Wu, C.-C., Aalders, J. W. G., van Duinen, R. J., Kester, D., & Wesselius, P. R. 1976, A&A, 50, 445
- Wu, C.-C., Panek, R. J., Holm, A. V., Schmitz, M., & Swank, J. H. 1983, PASP, 95, 391
- Yi, I., Narayan, R., Barret, D., & McClintock, J. E. 1996, A&A Supp., 120, 187

TABLE 1
JOURNAL OF OBSERVATIONS

	Start of Exposure (1998 UT Date/Time)		Object	Instrument	Wavelength Range (Å)	Obs. Time (s)
1	Mar 3	04:17:00	A0620-00	FLWO 1.2m	V	900
2*	Mar 4	05:35:03	A0620-00	HST/STIS	1700-3200	2150
3	Mar 4	06:67:55	A0620-00	HST/STIS	1700-3200	2550
4	Mar 4	08:35:06	A0620-00	HST/STIS	1700-3200	2550
5	Mar 4	10:11:55	A0620-00	HST/STIS	1700-3200	2550
6	Mar 4	11:48:43	A0620-00	HST/STIS	1700-3200	2550
7	Apr 1	09:43:15	Cen X-4	FLWO 1.2m	V	900
8	Apr 1	21:08:13	Cen X-4	HST/STIS	1700-3200	2150
9	May 5	03:09:01	A0620-00	HST/STIS	1700-3200	2150
10	May 5	04:40:25	A0620-00	HST/STIS	1700-3200	2550
11	May 5	06:17:35	A0620-00	HST/STIS	1700-3200	2550

*Spectrum not used in the present work because its “pipeline” background is a factor of ≈ 3 higher than for all the other spectra.

Fig. 1.— The summed spectrum of (a) A0620-00 ($T_{exp} = 4.8$ hrs) and the spectrum of (b) Cen X-4 ($T_{exp} = 0.6$ hrs). The spectra displayed here are binned at 2.0\AA and are not corrected for the effects of IS reddening. The strong line in both spectra is due to Mg II. Note that for A0620-00, the line is both very broad (2500 km s^{-1}) and single peaked.

Fig. 2.— A comparison of summed STIS spectra obtained two months apart. The change in intensity is modest. However, the errors have been reliably and conservatively determined, and we conclude that the continuum flux did decrease by a factor of $\approx 1.2 - 1.3$ during this two month period. The spectra have not been corrected for reddening.

Fig. 3.— The UV/optical continuum spectra of A0620-00 and Cen X-4. (a) Spectrum of A0620-00: The STIS data are plotted here as filled circles; each error bar is computed from the standard deviation of seven flux measurements. The data have been corrected for a reddening of $E_{B-V} = 0.35$. The STIS data are binned in 100\AA intervals with two exceptions: The highest frequency point is a 2σ upper limit averaged over a 300\AA band, and the adjacent data point is averaged over a 200\AA band. The lower/upper histograms represent the spectrum if one adopts a reddening of $E_{B-V} = 0.30/0.40$, rather than the nominal value of 0.35 . The 1992 FOS data (open squares) are taken from Table 1 in NMY96. An alternative optical spectrum of the non-stellar light, which was derived by Marsh et al. (1994), is indicated by the dashed line (see text). (b) Spectrum of Cen X-4: The STIS UV data are plotted as before for A0620-00. Here, however, the errors are those due to counting statistics (arbitrarily) multiplied by 3.0. The spectrum has been corrected for a nominal reddening of $E_{B-V} = 0.10$. The lower/upper histograms show the spectrum if one adopts a reddening of $0.05/0.15$.

Fig. 4.— Broadband spectra of A0620-00 and Cen X-4. The UV/optical data for both sources is the same as that shown in Figure 3. The EUV and X-ray data are discussed in the text. The ASCA X-ray upper limit in Figure 4a is at the 3σ level of confidence.

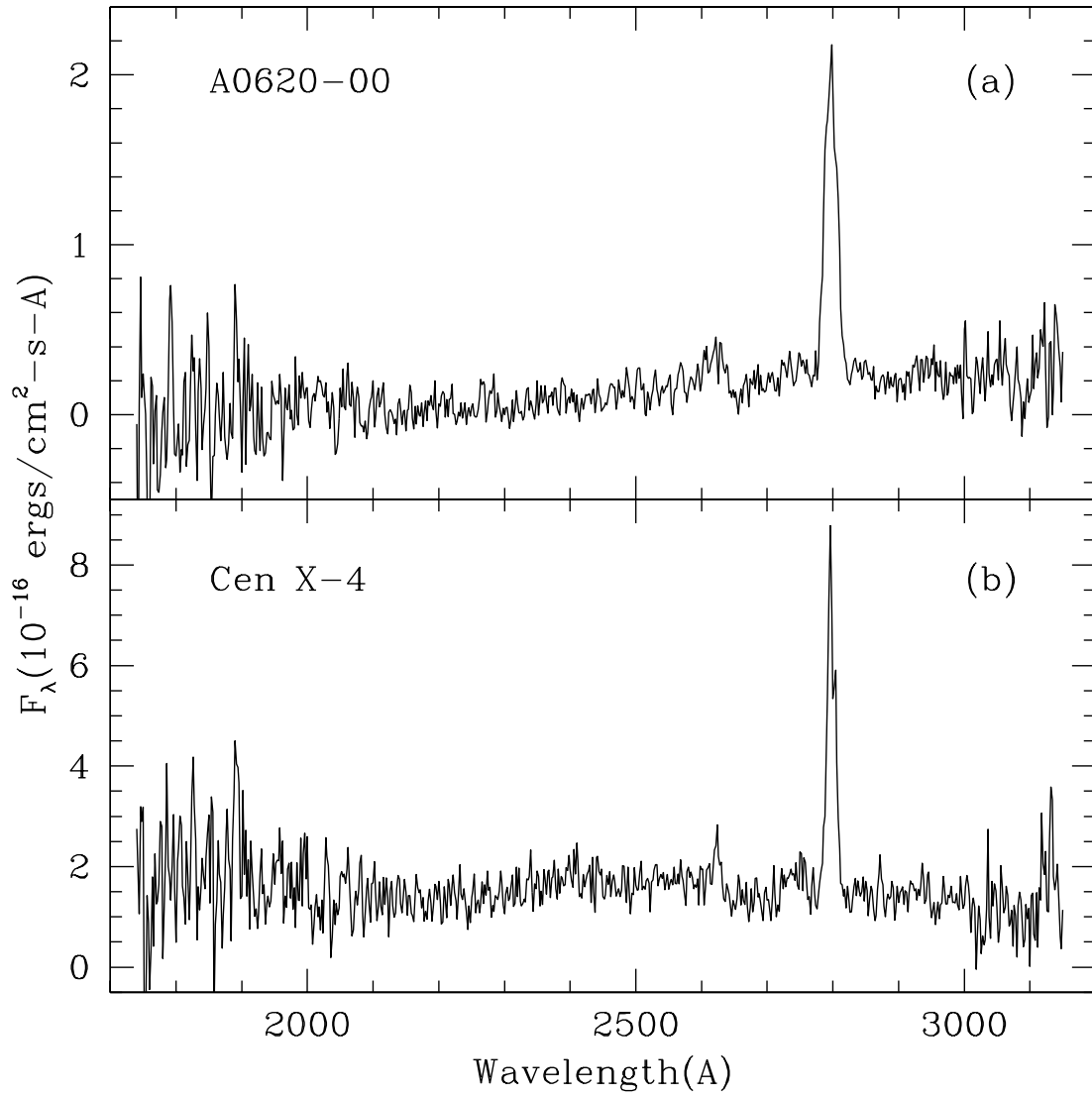


Fig. 1.—

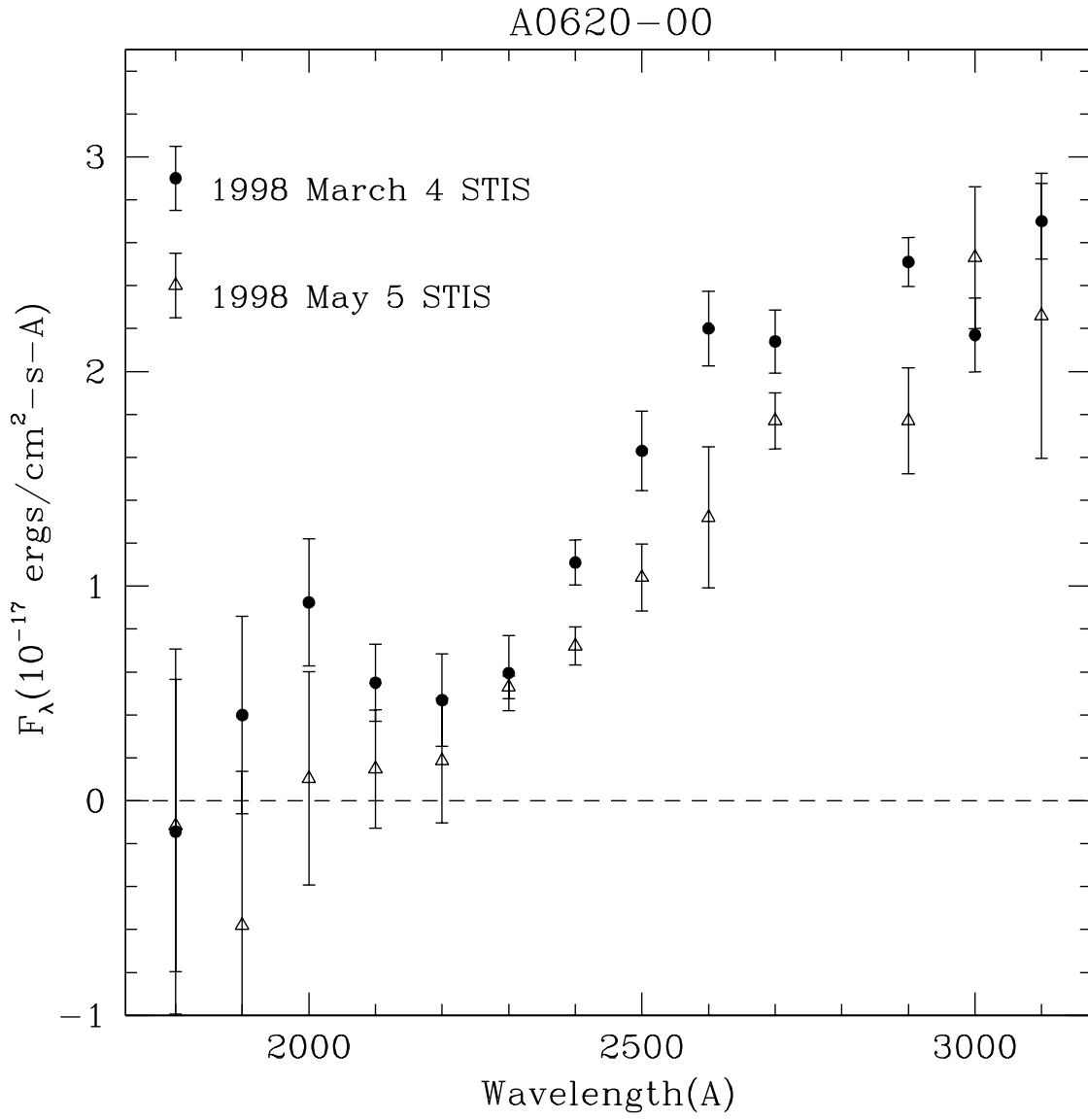


Fig. 2.—

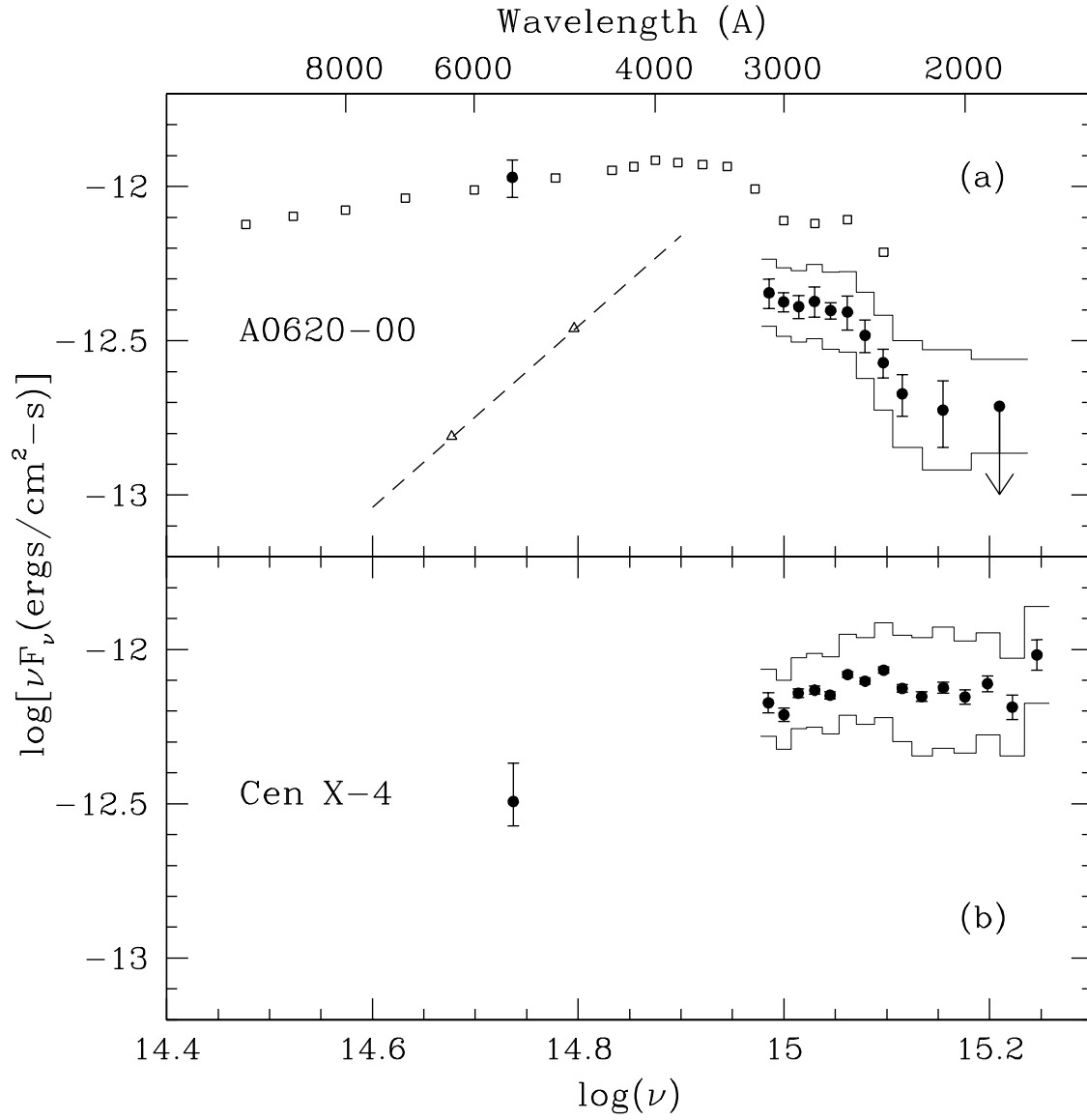


Fig. 3.—

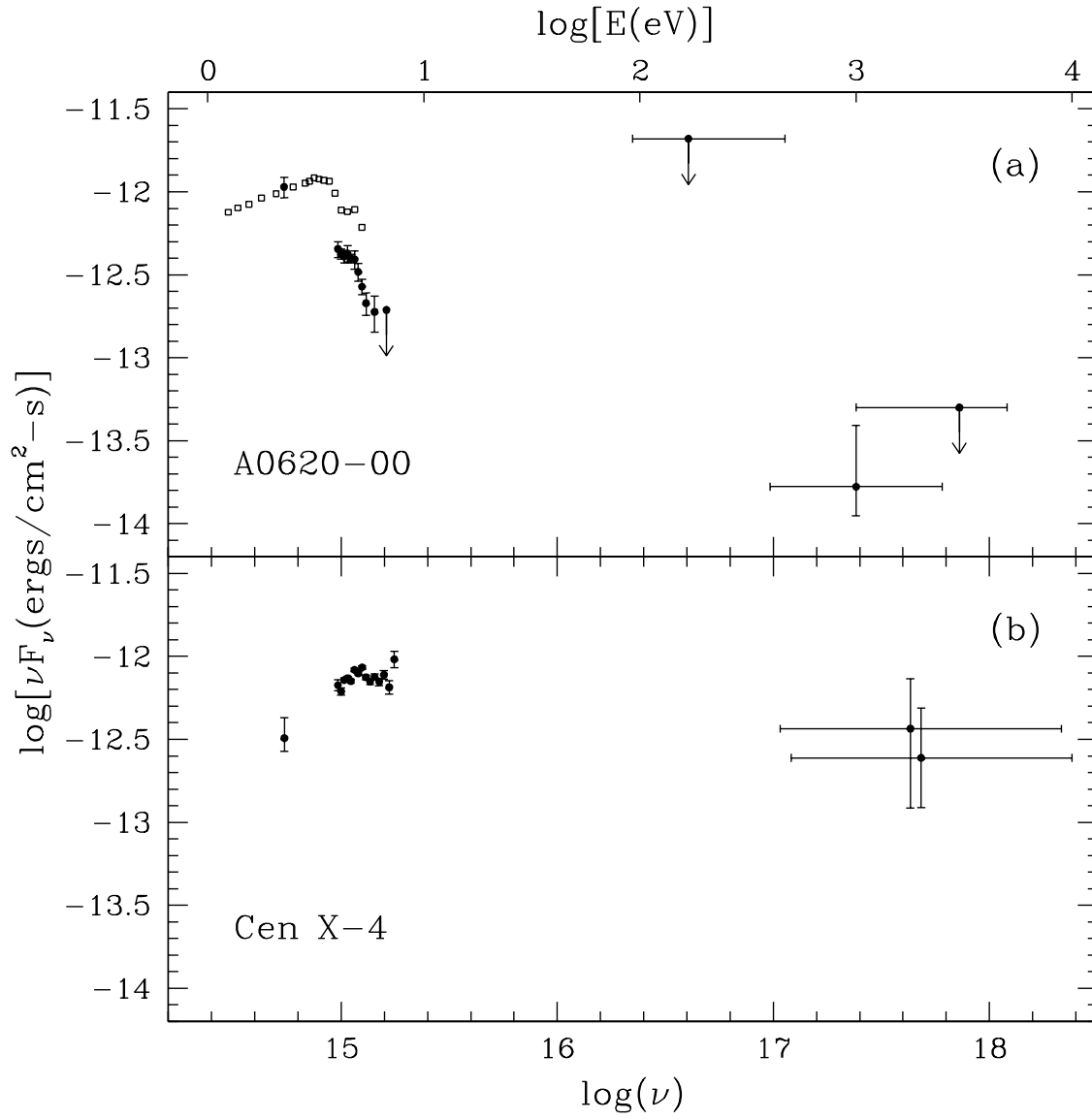


Fig. 4.—